

Preparing High-strength Ceramsite from Ferronickel Slag and Municipal Solid Waste Incineration Fly Ash

Xintao Wu¹, Foquan Gu^{1,2}, Chang Su¹, Wei Wang¹, Kai Pu¹, Dongsheng Shen^{1,2}, Yuyang Long^{1,2}

¹ Zhejiang Provincial Key Laboratory of Solid Waste Treatment and Recycling, School of Environmental Science and Engineering, Zhejiang Gongshang University, Hangzhou, Zhejiang 310012, China

² Instrumental Analysis Center of Zhejiang Gongshang University, Hangzhou, Zhejiang 310018, China

ABSTRACT

This study investigated the feasibility of preparing ceramsites from ferronickel slag and municipal solid waste incineration (MSWI) fly ash by evaluating the effect of adding MSWI fly ash on the phase and microstructure transformations and properties of ceramsites. The theoretical calculations indicated that when the addition of MSWI fly ash ranges from 10 wt.% to 60 wt.%, the main phases in the system are diopside, feldspar, forsterite and merwinite, all of which contribute to the improvement of ceramsites properties. The XRD and SEM analyses revealed that the initial phase of ferronickel slag and MSWI fly ash can be transformed into ceramsite phases during the roasting process. Specifically, forsterite and enstatite produced by the decomposition of olivine in ferronickel slag will react with calcium oxide produced by the decomposition of fly ash to form diopside and merwinite. Additionally, the reaction product will gradually change from diopside to merwinite as the MSWI fly ash addition increases. An excellent ceramsite with the cylindrical compressive strength significantly exceeding the requirements of high strength lightweight aggregates could be obtained by roasting the ferronickel slag with addition of 20 wt.% MSWI fly ash at 800 °C for pre-roasting 15 min and 1275 °C for roasting 20 min, demonstrating its remarkable application prospects in concrete.

1. INTRODUCTION

Ferronickel slag is produced during the production of Ni-Fe. It was estimated that the annual output of ferronickel slag to be greater than 40 million tons in China [1]. However, only approximately 10% of ferronickel slag is utilized in the construction industry, with the remainder is stored in the open air [2], which not only consumes a lot of land resources but also poses a serious underlying risk to environmental pollution. Due to the massive amount of ferronickel slag and the presence of harmful components (such as Cr, and Ni) [3], proper treatment of ferronickel slag is a complex problem that needs to be addressed for the sustainable development of the Ni-Fe industry.

The researchers' study focused on the production

of construction materials [4], geopolymers [5], glass ceramics and refractory materials [6-9], and recovering the valuable metals, i.e., Cr, Ni, Co etc. from ferronickel slag [10, 11]. Due to the low activity of ferronickel slag in construction materials, physical or chemical methods should be employed to activate the slag beforehand, although this pretreatment may limit the ferronickel slag dosage. Meanwhile, the high content of Cr in the slag significantly influences its dosage. The utilization of ferronickel slag to produce geopolymers and glass ceramics is hampered by disadvantages such as high cost and complex operation. It is feasible to prepare refractory materials from ferronickel slag, although the applications of the resulting refractory materials are rather limited. The cost of extracting valuable metals from ferronickel slag is considerably high since the slag's main components are MgO and SiO₂. Overall, resource utilization of ferronickel slag is still fraught with challenges.

In addition, municipal solid waste incineration (MSWI) has developed rapidly in China over the past decade. According to the National Bureau of Statistics, the total amount of municipal solid waste harmless treatment in China in 2020 was 0.23 billion tons, of which 0.15 billion tons were harmlessly treated by incineration [12]. MSWI has gradually become the main method to treat municipal solid waste in major cities. Unfortunately, around 3% to 10% of MSWI fly ash was produced during the incineration process, which contains high levels of dioxins and heavy metal and is a hazardous waste [13-15]. China was estimated to generate about 4.5-15 million tons of waste incineration fly ash in 2020. With the increase in the annual generation of MSWI fly ash, the pressure on the disposal of waste incineration fly ash also increases.

For treatment of MSWI fly ash, many efforts have been spent. Some studies examined the feasibility of cement-based stabilization/solidification for disposal in landfill [16, 17], recycling into construction materials [17, 18], and resource recovery (such as Zn, Pb, Cu, and Cd recovery) [19-21]. Among them, stabilization prior to landfill and cement kiln co-processing are currently two major approaches for treating MSWI fly ash [22]. However, due to the compatibility of

solidification/stabilization, the MSWI fly ash landfill occupies a significant amount of land resources. Alarmingly, there is still the risk of heavy metals dissolution during long-term landfilling [23]. As for the cement kiln co-processing method, high temperature process promotes the removal of dioxins from MSWI fly ash. However, due to the high Cl content in MSWI fly ash, additional dechlorination pretreatment [24], such as water washing, is necessary, however, the resulting effluent introduces secondary pollution problems. Meanwhile, in order to eliminate the influence of harmful elements such as Cl and heavy metals on cement-on-cement quality, the MSWI fly ash addition was strictly controlled in the cement kiln. In general, there are still numerous problems in the appropriate disposal of MSWI fly ash.

The main components of the ferronickel slag and MSWI fly ash are silica, magnesia, and calcium oxide, which have the potential to form ceramsite. Ceramsite has the advantages of high strength, good thermal insulation performance, excellent acid and alkali resistance, etc., and can be used as a good building aggregate [25-27]. Currently, the Chinese government restricts quarrying, advocates the use of solid waste as aggregate, and promotes comprehensive utilization of solid waste [28]. Therefore, the preparation of ceramsite from solid waste is expected to have promising future possibilities. Furthermore, during the process of ceramsite roasting, high temperatures can effectively solidify harmful substances such as heavy metals in MSWI fly ash [29-31], and the decomposition of organic matter in MSWI fly ash aids ceramsite in forming a porous structure. This strategy can not only eliminate the pollution concerns caused by ferronickel slag and MSWI fly ash, but it can also leverage the properties of ferronickel slag and MSWI fly ash to improve the performance of ceramsite.

In the present study, the phase and microstructure transformation behaviors of the ferronickel slag and fly ash systems were revealed based on the theoretical calculations, TG-DSC analysis, XRD analysis and SEM analysis under the condition of different MSWI fly ash additions, and the feasibility for preparing ceramsite from ferronickel slag and MSWI fly ash was verified. The findings are intended to provide an efficient and straightforward technological route for the resource utilization of ferronickel slag and MSWI fly ash.

2. EXPERIMENTAL

2.1. Materials

The ferronickel slag sample was a submerged arc furnace slag from the production of Ni-Fe alloy [32]. As showed in Table 1, the ferronickel slag was characterized by high contents of silica (48.29 wt.%) and magnesia (30.95 wt.%). The concentration of Zn, Pb, Cu, Cr, and Ni in ferronickel slag was 3023.09 mg/kg, 329.98 mg/kg, 528.57 mg/kg, 8135.65 mg/kg,

and 909.38 mg/kg, respectively. The MSWI fly ash sample from flue gas treatment system of the municipal waste incineration plant. The MSWI fly ash contained 64.34 wt.% lime, 16.34 wt.% chlorine, 4.74 wt.% potassium oxide, 3.81 wt.% sodium oxide, 2.72 wt.% sulphur trioxide, and 2.50 wt.% silica. The concentration of Zn, Pb, Cu, Cd, Cr, and Ni in MSWI fly ash was 8558.58 mg/kg, 2039.57 mg/kg, 656.71 mg/kg, 292.14 mg/kg, 55.30 mg/kg and 17.25 mg/kg, respectively. The heavy metals leaching concentration of Pb, Zn, Cu, Cr, and Ni in MSWI fly ash was 18.91 mg/L, 3.07 mg/L, 0.02 mg/L, 0.36 mg/L and 0.14 mg/L, respectively. The heavy metals leaching concentration of Cr in ferronickel slag was 0.03 mg/L. The heavy metals leaching concentration of Pb in MSWI fly ash exceeds the limit of the Chinese national identification standards for hazardous wastes-identification for extraction toxicity (GB 5085.3-2007) [33]. The main phase of ferronickel slag was olivine, the main phase of MSWI fly ash was CaCO_3 , CaOHCl , NaCl , Ca(OH)_2 and KCl .

2.2 Methods

2.2.1. Thermodynamic analysis: The FactSage 8.0 software was used to evaluate the influence of MSWI fly ash on the phase transformation of ferronickel slag by calculating the thermodynamic equilibrium phase content of the ferronickel slag and MSWI fly ash system under different temperature conditions.

2.2.2. Experimental procedure: At first, the ferronickel slag was ground to a particle size of less than 74 μm , and then mixed with MSWI fly ash according to the corresponding mass ratio. After adding suitable water, the mixture was granulated into pellets with a diameter of 12 mm. After dried at 105 $^{\circ}\text{C}$ for 12 h, the dried pellets were pre-roasted in an electric furnace at 800 $^{\circ}\text{C}$ for 15 min, and then roasted at 1275 $^{\circ}\text{C}$ for 20 min. After cooled down naturally in the furnace to 25 $^{\circ}\text{C}$, the ceramsite was taken out for the subsequent analysis and performance characterization.

2.2.3. Instrumental analysis and performance characterization: The elemental composition of samples was analyzed by X-ray fluorescence (XRF; XRF-1800, Japan Shimadzu FEI Co., Ltd). The concentration of heavy metals in samples were determined by atomic absorption spectrometer (AAS, ICE 3500, USA Thermo Fisher Scientific Co., Ltd). The decomposition properties and thermodynamic characteristics of the samples during roasting were identified by a simultaneous thermal analyzer (DSC-TGA, SDT 650, TA Instruments Co., Ltd) in the temperature range from 25 $^{\circ}\text{C}$ to 1400 $^{\circ}\text{C}$ with a ramp rate of 10 $^{\circ}\text{C}/\text{min}$ in air. The phase compositions of the ceramsites were tested by an X-ray diffractometer (XRD, D8 Advance, Germany Bruker Co., Ltd) with a copper target. The microstructure and compositions of the ceramsites were analyzed by a scanning electron

microscope (SEM, FEI QUANTA 200, FEI Co., Ltd). The pore distribution of ceramsite were determined by an automatic mercury porosimeter (AutoPore 9620, USA Micromeritics Co., Ltd), and the sample size used for testing was 10 mm×10 mm×10 mm.

The properties of the obtained ceramsite were characterized according to the Chinese National Standard Test Methods (GB/T17431.2-2010) [34]. The leaching behavior of zinc, lead, copper, cadmium, chromium, and nickel in the MSWI fly ash and ceramsite samples was analyzed based on the Chinese Solid Waste Extraction Procedure for Leaching Toxicity- Sulphuric acid & nitric acid method (HJ/T 299-2007) [35].

3. RESULTS AND DISCUSSION

3.1. Thermodynamic analysis

The effect of MSWI fly ash addition on the phase evolution of ferronickel slag was revealed by evaluating the transformation behavior of the thermodynamic equilibrium phase content of ferronickel slag and MSWI fly ash system at 1275 °C. This can be seen from Fig. 1 that increasing MSWI fly ash addition, resulted in a significant difference in the phase content of the system presented a significant difference. Specifically, when the addition of MSWI fly ash of 10 wt.%, the system contained 28.15% forsterite, 28.09% diopside, 19.70% enstatite, 11.40% hematite and 12.66% feldspar. When the addition of MSWI fly ash of 20 wt.%, the liquid phase began to appear, and the system mainly included 33.30% forsterite, 30.35% diopside, 24.42% feldspar, 10.83% hematite, and 1.10% liquid. With the addition of MSWI fly ash increased to 30 wt.%-60 wt.%, the diopside and forsterite were gradually replaced by merwinite, with diopside disappearing at 30 wt.%, forsterite disappearing at 60 wt.%. With the addition of MSWI fly ash further increased to 70 wt.%-100 wt.%, merwinite disappeared and lime increased substantially, a large amount of free lime in the system will affect the stability of ceramsite. As the addition of MSWI fly ash reaches 100 wt.%, the system comprised 66.04% lime, 16.18% liquid, 8.45% Ca_2SiO_4 , 5.39% CaSO_4 , 3.94% $\text{Ca}_2\text{Fe}_2\text{O}_5$ and $\text{Ca}_3\text{MgAl}_4\text{O}_{10}$. It should be noted that as the percentage of MSWI fly ash increased from 20 wt.% to 100 wt.%, the content of liquid increased from about 1.10% to 16.20%. The formation of liquid in the system may promote roasting and increase the strength of ceramsite. In summary, the appropriate addition of MSWI fly ash is 20 wt.%-60 wt.%, however this must yet be determined by further experiments.

3.2. Phase and microstructure transformations of ferronickel slag and MSWI fly ash system during roasting

Phase and microstructure transformations of

ferronickel slag and MSWI fly ash system during roasting was explored by XRD and SEM analyses.

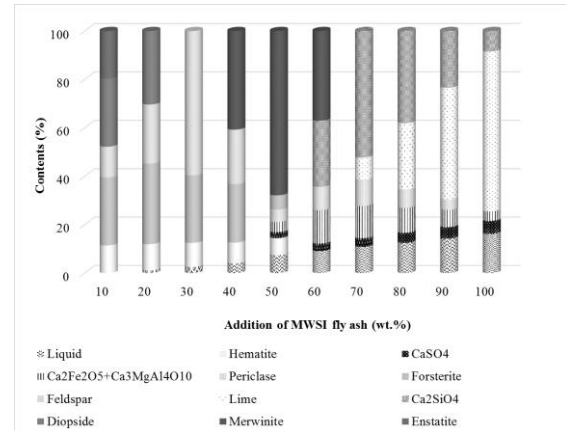


Fig. 1. Calculated contents of thermodynamic equilibrium phases in the ferronickel slag and MSWI fly ash system with different additions of MSWI fly ash.

3.2.2. XRD analysis The XRD results of the resulting ceramsite produced by roasting ferronickel slag with 10 wt.%-50 wt.% MSWI fly ash is shown in Fig. 2. The phases of the ceramsite obtained with 10 wt.% MSWI fly ash were diopside ($\text{CaMgSi}_2\text{O}_6$), feldspar, forsterite (Mg_2SiO_4), and enstatite (MgSiO_3). Increasing the MSWI fly ash addition to 20 wt.%, the intensity of the enstatite diffraction peaks decreased, and the main phases of the obtained ceramsite were diopside, feldspar and forsterite. With the MSWI fly ash addition increased to 30 wt.%, merwinite ($\text{Ca}_2\text{MgSi}_2\text{O}_7$) and quartz diffraction peaks appeared, while the intensity of diopside diffraction peaks decreased, diopside, merwinite, feldspar, forsterite and quartz were the main phases of the obtained ceramsite. Further increasing the MSWI fly ash addition to 50 wt.%, the phase of the ceramsite remained unchanged, but the intensity of diopside and forsterite diffraction peaks gradually decreased, while the intensity of merwinite diffraction peaks increased dramatically. The transformation of the main phases agreed well with the calculate results in Fig. 3. It is apparent shows that the original phase undergoes a complex chemical reaction during the roasting process. The relevant reactions are depicted in Equations (1)-(9). At about 800 °C, the olivine in the ferronickel slag decomposed to Mg_2SiO_4 , SiO_2 , and Fe_2O_3 (Equation (1)). During the roasting process, the CaCO_3 , Ca(OH)_2 , and CaOHCl in MSWI fly ash decomposed to CaO (Equations (2)-(4)). The generated Mg_2SiO_4 , SiO_2 and CaO further reacted to form $\text{CaMgSi}_2\text{O}_6$ and $\text{Ca}_2\text{MgSi}_2\text{O}_7$ (Equations (5)-(6)). In addition, Mg_2SiO_4 and SiO_2 can react to form MgSiO_3 (Equation (7)), and the resulting MgSiO_3 , SiO_2 , and CaO can also be further reacted to form $\text{CaMgSi}_2\text{O}_6$ and $\text{Ca}_2\text{MgSi}_2\text{O}_7$ (Equations (8)-(9)). As

the content of CaO in the system increases, the reaction product gradually changes from $\text{CaMgSi}_2\text{O}_6$ to $\text{Ca}_2\text{MgSi}_2\text{O}_7$ (Equation (10)), this explains the significantly increased merwinite diffraction peak intensity and the continuously decreasing diopside diffraction peak intensity in the ceramsites as the MSWI fly ash addition exceeds 40 wt.%. It was reported that during the diopside formation process, heavy metals (such as Zn, Cu, and Pb) could be substituted to magnesium (II) or calcium (II) to form the new components, thereby immobilizing the heavy metals in the crystal lattice of the new mineral. Besides, the calcium-containing mineral has been considered to be easy to form a high-strength structure [30]. As a result, ceramsites with diopside as the primary phase may characterize by high-strength and a great ability to immobilize heavy metals. In addition, unlike MSWI fly ash, no chlorine-containing minerals were found in the ceramsites, because chlorine-containing compounds easily decompose and volatilize into gases during the high-temperature roasting process. It should be noted that, in contrast to the thermodynamic equilibrium phase calculation results, no Fe-bearing minerals were found in the ceramsites as some iron may remain in the olivine phase formation of the iron-rich forsterite or substituted with $\text{Mg}^{2+}/\text{Ca}^{2+}$ appeared in the diopside, merwinite, and feldspar phase.

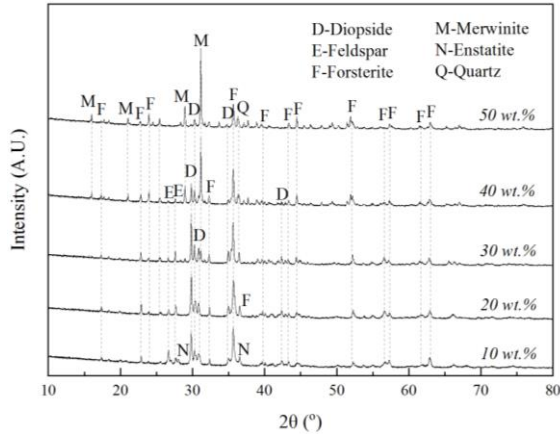
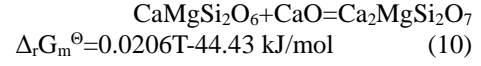
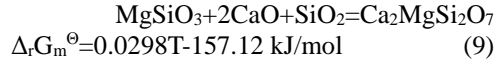
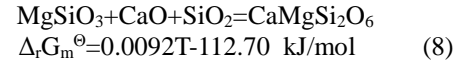
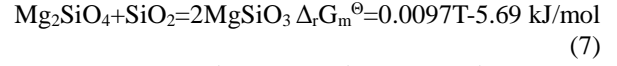
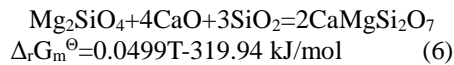
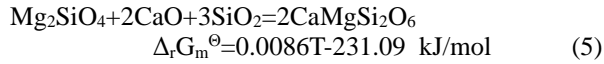
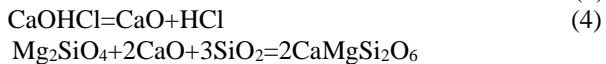
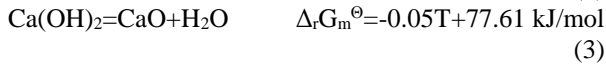
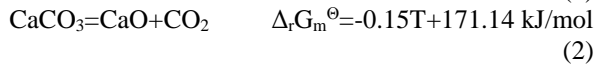
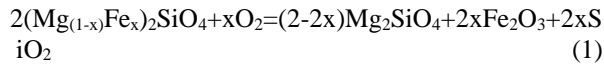


Fig. 2. XRD patterns of ceramsites roasted with different additions of MSWI fly ash.



3.2.2. SEM analysis Furthermore, the micro-morphologies of the ceramsites were analyzed using SEM. Fig. 3 shows SEM images of the ceramsite generated by roasting ferronickel slag with the addition of 10 wt.%-50 wt.% MSWI fly ash at 800 °C for 15 min pre-roasting and 1275 °C for 20 min roasting. As illustrated in Fig. 3, when the addition of MSWI fly ash was at 10 wt.%-20 wt.%, the ceramsites contained a modest amount of evenly distributed pores surrounded by a significant amount of crystal phases formed during the roasting process, with the majority of pores filled by the liquid phase generated during the roasting process. This not only helps to promote the roasting process and improve the strength of the ceramsite, but also reduces water absorption of the ceramsite and promotes the solidification of heavy metals. According to the mercury intrusion porosimetry results, the total pore area and average pore diameter of the ceramsite (MSWI fly ash addition of 20 wt.%) were 0.062 m²/g and 4.26 μm. However, as the amount of MSWI fly ash addition increased, the pores gradually expanded and penetrated into wide open pores, which is harmful to the compressive strength and water absorption rate densification of the ceramsite.

3.3. Properties of ceramsites

The effect of MSWI fly ash on the bulk density, apparent density, cylindrical compressive strength and 1-h water absorption rate of the obtained ceramsite was investigated when the ferronickel slag was pre-roasted at 800 °C for 15 min and roasted at 1275 °C for 20 min with different MSWI fly ash additions. The results shown in Fig. 4 reveal that when 10 wt.%-20 wt.% of MSWI fly ash were added, the bulk density, apparent density, cylindrical compressive strength, and 1-h water absorption rate of the obtained ceramsite were similar, and exhibited extremely high cylindrical compressive strength (36.80 MPa-37.50 MPa). However, as the addition of MSWI fly ash increased, the cylindrical compressive strength of the obtained ceramsite declined significantly. In contrast, 1-h water absorption rate of the ceramsite increased rapidly, while the bulk density and apparent density showed a trend of first decreasing and then increasing. It is evident that the addition of MSWI fly ash leads to a significant decrease in bulk density and cylindrical compressive strength, which is due to the decomposition of carbonates, and the volatilization of heavy metal chlorides and salts in the MSWI fly ash during the roasting process [36]. At the

same time, the particles of ceramsite become smaller, due to the decomposition and volatilization of these substances, which was the reason for the ceramsite bulk density, apparent density starts to increase after the addition of MSWI fly ash exceeds 60%. It should be noted that the 1-h water absorption of ceramsite decreased when the addition of MSWI fly ash reaches 80 wt.%, which was due to the loose ceramsite structure and certain components being dissolved during the water absorption experiment. When the addition of MSWI fly ash reaches 90 wt.%, the dissolution phenomenon became more severe, and the ceramsite was entirely disintegrated in water.

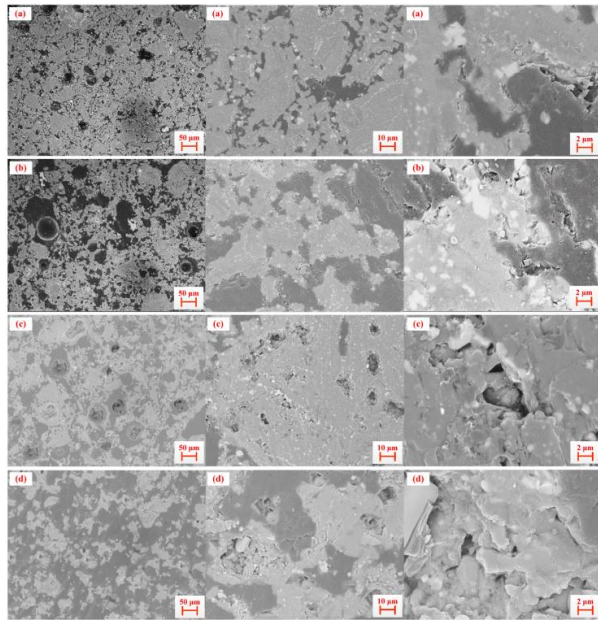


Fig. 3. SEM images of the ceramsites obtained with different additions of MSWI fly ash: (a) MSWI fly ash addition of 10 wt.%, (b) MSWI fly ash addition of 20 wt.%, (c) MSWI fly ash addition of 30 wt.%, and (d) MSWI fly ash addition of 50 wt.%.

Given the high Pb and Zn leaching concentrations and Cl content of MSWI fly ash, the Pb and Zn leaching concentrations and Cl content of ceramsites were examined to evaluate environmental safety. As shown in Table 3, the Zn leaching concentration in ceramsites was all below the detection limit with the MSWI fly ash addition reaching 10 wt.%-90 wt.%, indicating effective stabilization in ceramsites. When the MSWI fly ash addition reaches 10 wt.%-80 wt.%, the Pb leaching concentration in ceramsites remains low and can meet the requirements of the Chinese National Integrated Wastewater Discharge Standard (GB 8978-1996) [37]. When the MSWI fly ash addition reaches 10 wt.%, no Cl was found in ceramsite. However, as the addition of MSWI fly ash increased, so did the content of Cl in ceramsites. When the addition

of MSWI fly ash is below 40 wt.%, the Cl content can meet the requirements of pollution control [38].

Table 1. Pb and Zn leaching concentration and Cl content of the ceramsites.

Addition of						
MSWI fly ash	10	20	30	50	60	80
(wt.%)						
Pb leaching						
concentration	0.004	0.007	0.02	0.02	0.01	0.02
(mg/L)						
Zn leaching						
concentration	ND	ND	ND	ND	ND	ND
(mg/L)						
Cl content	ND	0.08	1.33	2.46	3.30	9.46
(wt.%)						

Based on the above analysis, a good ceramsite with bulk density of 1205 kg/m³, apparent density of 2249 kg/m³, cylindrical compressive strength of 36.80 MPa and 1-h water absorption rate of 6.15% can be obtained by roasting the ferronickel slag with the addition of 20 wt.% MSWI fly ash at 800 °C for pre-roasting 15 min and at 1275 °C for roasting 20 min. The obtained ceramsite basically met the quality standard of ceramsite products of GB/T17431.1-2010 [39], and the cylindrical compressive strength far exceeds the requirements of high strength lightweight aggregates, showing its great application potential in concrete.

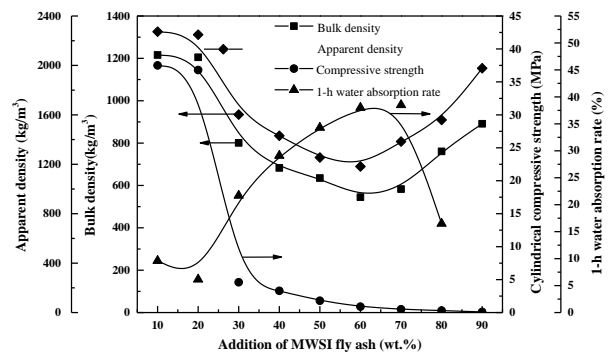


Fig. 4. Effect of addition of MSWI fly ash on the bulk density, apparent density, cylindrical compressive strength and 1-h water absorption rate of the ceramsite.

4. CONCLUSIONS

This study validated the feasibility of preparing ceramsites from ferronickel slag and MSWI fly ash was

verified in this study. The results of theoretical equilibrium phase content of ferronickel slag and MSWI fly ash system at 1275 °C revealed that with the MSWI fly ash addition of 10 wt.%-60 wt.%, the main phases in the system were diopside, feldspar, forsterite, and merwinite were, which contributed to improving the performance of ceramsites. With the addition of MSWI fly ash further increased to 70 wt.%-100 wt.%, a large amount of free lime generated in the system will impair the stability of ceramsite. The TG-DSC results indicated that the appropriate addition of MSWI fly ash contributed to decrease the smelting point of the ferronickel slag system, which is expected to promote the roasting process. XRD and SEM analyses indicated that the original phase of ferronickel slag and MSWI fly ash could be transformed to ceramsite phases during the roasting process. Specifically, forsterite and enstatite generated from the decomposition of olivine in ferronickel slag will react with calcium oxide produced by the decomposition of fly ash to form diopside and merwinite, and as the addition of MSWI fly ash increases, the reaction product will gradually change from diopside to merwinite. The experimental results exhibited that a great ceramsite with bulk density of 1205 kg/m³, apparent density of 2249 kg/m³, cylindrical compressive strength of 36.80 MPa and 1-h water absorption rate of 6.15% could be obtained by roasting the ferronickel slag with the addition of 20 wt.% MSWI fly ash at 800 °C for 15 min pre-roasting and 1275 °C for 20 min roasting. In general, the proposed technological route has the characteristics of simple operation and high efficiency is expected to be widely adopted in the simultaneous utilization of ferronickel slag and MSWI fly ash.

ACKNOWLEDGEMENTS

This work was partially supported by the Key R&D Program of Zhejiang Province, China (2020C03086, 2022C03059), the Scientific Research Project of Zhejiang Provincial Department of Education (Y202147303), and the Undergraduate Training Program on Innovation and Entrepreneurship of Zhejiang Gongshang University (CX202223005, CX202223010).

REFERENCES

- [1] F. Gu, Y. Zhang, Z. Peng, H. Tang, M. Lu, S. Liu, Z. Su, M. Rao, G. Li and T. Jiang. Recovery of chromium from ferronickel slag via alkaline roasting followed by water leaching: effect of roasting atmosphere, Z. Peng et al. (eds.), 11th International Symposium on High-Temperature Metallurgical Processing, The Minerals, Metals & Materials Series (2020) 359-367.
- [2] Y. Huang, Q. Wang, M. Shi, Characteristics and reactivity of ferronickel slag powder, Constr. Build. Mater. 156 (2017) 773-789.
- [3] F. Gu, Y. Zhang, Z. Su, Y. Tu, S. Liu, T. Jiang, Recovery of chromium from chromium-bearing slags produced in the stainless-steel smelting: A review, J. Clean Prod. 296 (2021) 126467.
- [4] M. Nuruzzaman, J. C. Kuri, P. K. Sarker, Strength, permeability and microstructure of self-compacting concrete with the dual use of ferronickel slag as fine aggregate and supplementary binder, Constr. Build. Mater. 318 (2022) 125927.
- [5] J.C. Kuri, P.K. Sarker, F.U.A. Shaikh, Sulphuric acid resistance of ground ferronickel slag blended fly ash geopolymer mortar, Constr. Build. Mater. 313 (2021) 125505.
- [6] W. Shang, Z. Peng, F. Xu, H. Tang, M. Rao, G. Li, T. Jiang, Preparation of enstatite-spinel based glass-ceramics by co-utilization of ferronickel slag and coal fly ash, Ceram. Int. 47 (2021) 29400-29409.
- [7] L. Yang, Z. Peng, Y. Huang, L. Wang, L. Zheng, M. Rao, G. Li, T. Jiang, Co-utilization of ferronickel slag and fly ash cenosphere for production of superior thermal insulation materials, Ceram. Int. 47 (2021) 10019-10026.
- [8] H. Tang, Z. Peng, F. Gu, L. Yang, W. Tian, Q. Zhong, M. Rao, G. Li, T. Jiang. Chromium-promoted preparation of forsterite refractory materials from ferronickel slag by microwave sintering, Ceram. Int. 47 (2021) 10809-10818.
- [9] F. Gu, Y. Zhang, Y. Tu, X. Wu, Y. Zhu, Y. Long, D. Shen, Assessing magnesia effect on preparing refractory materials from ferrochromium slag, Ceram. Int. 48 (2022) 13100-13107.
- [10] Z. Peng, L. Wang, F. Gu, H. Tang, M. Rao, Y. Zhang, G. Li, T. Jiang, Recovery of chromium from ferronickel slag: A comparison of microwave roasting and conventional roasting strategies, Powder. Technol. 372 (2020) 578-584.
- [11] F. Gu, Y. Zhang, Z. Peng, Z. Su, H. Tang, W. Tian, G. Liang, Joonho Lee, M. Rao, G. Li, T. Jiang, Selective recovery of chromium from ferronickel slag via alkaline roasting followed by water leaching, J. Hazard. Mater. 374 (2019) 83-91.
- [12] <https://data.stats.gov.cn/search.htm?s=%E5%9E%83%E5%9C%BE>.
- [13] C. Zhao, S. Lin, Y. Zhao, K. Lin, L. Tian, M. Xie, T. Zhou, Comprehensive understanding the transition behaviors and mechanisms of chlorine and metal ions in municipal solid waste incineration fly ash during thermal treatment, Sci. Total. Environ. 807 (2022) 150731.
- [14] P. Ren, T. Ling, K. Mo. CO₂ pretreatment of municipal solid waste incineration fly ash and its feasible use as supplementary cementitious material, J. Hazard. Mater. 424 (2022) 127457.
- [15] Y. Mao, H. Wu, W. Wang, M. Jia, X. Che.

- Pretreatment of municipal solid waste incineration fly ash and preparation of solid waste source sulphoaluminate cementitious material, *J. Hazard. Mater.* 385 (2020) 121580.
- [16] C. Fan, B. Wang, T. Zhang. Review on cement stabilization/solidification of municipal solid waste incineration fly ash. *Adv. Mater. Sci. Eng.* 2018 (2018) 1-7.
- [17] S. Zhao, F. Muhammad, L. Yu, M. Xia, X. Huang, B. Jiao, N. Lu, D. Li, Solidification/stabilization of municipal solid waste incineration fly ash using uncalcined coal gangue-based alkali-activated cementitious materials. *Environ. Sci. Pollut. Res.* 26 (2019) 25609-25620.
- [18] J. Li, S. Zhang, Q. Wang, W. Ni, K. Li, P. Fu, W. Hu, Z. Li. Feasibility of using fly ash-slag-based binder for mine backfilling and its associated leaching risks. *J. Hazard. Mater.* 400 (2020) 123191.
- [19] Y. Zhang, L. Wang, L. Chen, B. Ma, Y. Zhang, W. Ni, D.C.W. Tsang. Treatment of municipal solid waste incineration fly ash: State-of-the-art technologies and future perspectives. *J. Hazard. Mater.* 411 (2021) 125132.
- [20] C. Geng, J. Liu, S. Wu, Y. Jia, B. Du, S. Yu. Novel method for comprehensive utilization of MSWI fly ash through co-reduction with red mud to prepare crude alloy and cleaned slag, *J. Hazard. Mater.* 384 (2020) 121315.
- [21] K. Kurashima, K. Matsuda, S. Kumagai, T. Kameda, Y. Saito, T. Yoshioka. A combined kinetic and thermodynamic approach for interpreting the complex interactions during chloride volatilization of heavy metals in municipal solid waste fly ash, *Waste Manag.* 87 (2019) 204-217.
- [22] Kanhar A. H., S. Chen, F. Wang, Incineration fly ash and its treatment to possible utilization: A review, *Energies* 13 (2020) 6681.
- [23] X. Tian, F. Rao, C. Li, W. Ge, N.O. Lara, S. Song, L. Xia, Solidification of municipal solid waste incineration fly ash and immobilization of heavy metals using waste glass in alkaline activation system, *Chemosphere* 283 (2021) 131240.
- [24] X. Wang, M. Wang, D. Zou, C. Wu, T. Li, M. Gao, S. Liu, Q. Wang, T. Shimaoka, Comparative study on inorganic Cl removal of municipal solid waste fly ash using different types and concentrations of organic acids, *Chemosphere* 261 (2020) 127754.
- [25] T. Ji, D. Zheng, X. Chen, X. Lin, H. Wu, Effect of prewetting degree of ceramsite on the early-age autogenous shrinkage of lightweight aggregate concrete, *Construct. Build. Mater.* 98 (2015) 102-111.
- [26] X. Zheng, T. Ji, S.M. Easa, B. Zhang, Z. Jiang, Tensile basic creep behavior of lightweight aggregate concrete reinforced with steel fiber, *Construct. Build. Mater.* 200 (2019) 356-367.
- [27] X. Li, P. Wang, J. Qin, Y. Liu, Y. Qu, J. Liu, R. Cao, Y. Zhang, Mechanical properties of sintered ceramsite from iron ore tailings affected by two-region structure, *Construct. Build. Mater.* 240 (2020) 117919.
- [28] L. Luo, X. Tu, Z. Peng, Preparation and heavy metals solidification of ceramsite from lake mud, *Bull. Chin. Ceram. Soc.* 38 (2019) 3397-3402 (In Chinese).
- [29] Y. Long, J. Qiu, Q. Bao, F. Gu, Z. Wu, M. Wu, W. Guo, D. Shen, Effect of Fe_2O_3 on the leaching behavior of Cr in hazardous waste incineration fly ash after thermal treatment, *Environ. Technol. Inno.* 24 (2021) 102072.
- [30] X. Zhan, L. Wang, L. Wang, J. Gong, X. Wang, X. Song, T. Xu, Co-sintering MSWI fly ash with electrolytic manganese residue and coal fly ash for lightweight ceramsite, *Chemosphere* 263 (2021) 127914.
- [31] H. Mi, L. Yi, Q. Wu, J. Xia, B. Zhang, Preparation of high-strength ceramsite from red mud, fly ash, and bentonite, *Ceram. Int.* 47 (2021) 18218-18229.
- [32] F. Gu, Z. Peng, Y. Zhang, H. Tang, L. Ye, W. Tian, G. Liang, M. Rao, G. Li, T. Jiang, Facile route for preparing refractory materials from ferronickel slag with addition of magnesia, *ACS Sustainable Chem. Eng.* 6 (2018) 4880-4889.
- [33] China National Environmental Protection Administration and General Administration of Quality Supervision, Inspection and Quarantine of the People's Republic of China, Identification standards for hazardous wastes-identification for extraction toxicity, China Environmental Science Press, Beijing, 2007.
- [34] General Administration of Quality Supervision, Inspection and Quarantine of the People's Republic of China and China Standardization Administration, Lightweight aggregates and its test methods—Part 2: Test methods for lightweight aggregates, Standards Press of China, Beijing, 2010.
- [35] China National Environmental Protection Administration, Solid Waste Extraction Procedure for Leaching Toxicity Acetic Acid Buffer Solution Method, China Environmental Science Press, Beijing, 2007.
- [36] M. Liu, C. Wang, Y. Bai, G. Xu, Effects of sintering temperature on the characteristics of lightweight aggregate made from sewage sludge and river sediment, *J. Alloys Compd.* 748(2018), 522-527.
- [37] The State Bureau of Quality and Technical Supervision, Integrated wastewater discharge standard, Standards Press of China, Beijing, 1996.
- [38] Ministry of Ecological Environment of the People's Republic of China, technical specification for pollution control of fly-ash from municipal

solid waste incineration, China Environmental Science Press, Beijing, 2020.

- [39] General Administration of Quality Supervision, Inspection and Quarantine of the People's Republic of China and China Standardization Administration, Lightweight aggregates and its test methods—Part 1: Lightweight aggregates, Standards Press of China, Beijing, 2010.